Computational model of polarized actin cables and cytokinetic actin ring formation in budding yeast

Haosu Tang, Tamara C. Bidone, Dimitrios Vavylonis

Supplementary Figures and Movies

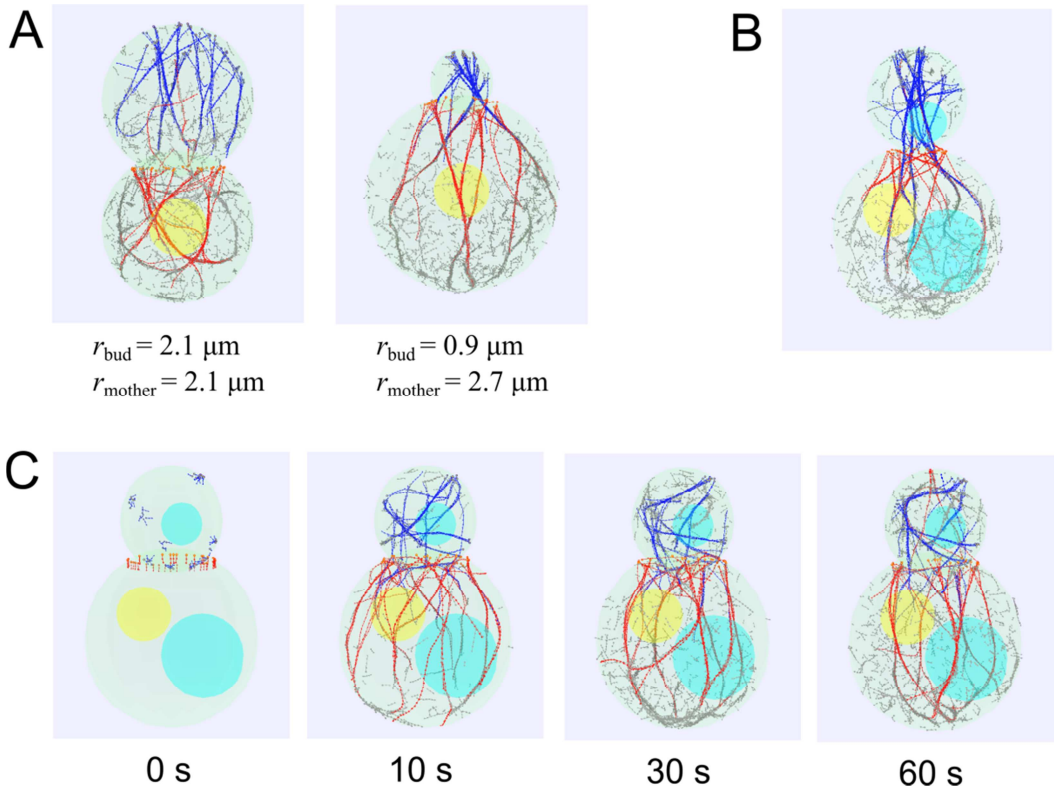

Figure S1. Simulation results with modified cell geometry, Bni1/Bnr1 polymerization rate and Bni1 localization. (A) Cable structure is robust to changes in bud/mother size. Left: Simulation snapshot of big bud centered at (0,0,3.5) with radius 2.1 and small mother cell centered at (0,0,0) with radius 2.1 (units: µm). Neck radius: 1.16 µm. Right: Simulation snapshot of small bud centered at (0,0,3.1) with radius 0.9 and big mother cell centered at (0,0,0) with radius 2.7 (units: µm). Neck radius: 0.75 µm. (B) Simulation with larger polymerization rate for Bni1filaments compared to Bnr1, r_{Bni1} = 0.6 µm/s, r_{Bnr1} = 0.3 µm/s (the reference parameter set has r_{Bni1} = 0.3 µm/s, r_{Bnr1} = 0.6 µm/s). Bni1 cables go through the neck and bundle with Bnr1 cables. Fewer cables can reach all the way down to the bottom compared to the reference case. Simulation snapshot is taken at 60 s. Neck radius**:** 0.54 µm. (C) Simulation with Bni1 clusters randomly distributed around the bud surface rather than just at the bud tip as in the reference case. More Bni1-associated actin filaments remain in the bud, forming a slightly more complex network than in Figure 2. The structure of Bnr1-associated cables in the mother cell does not differ significantly from the reference case.

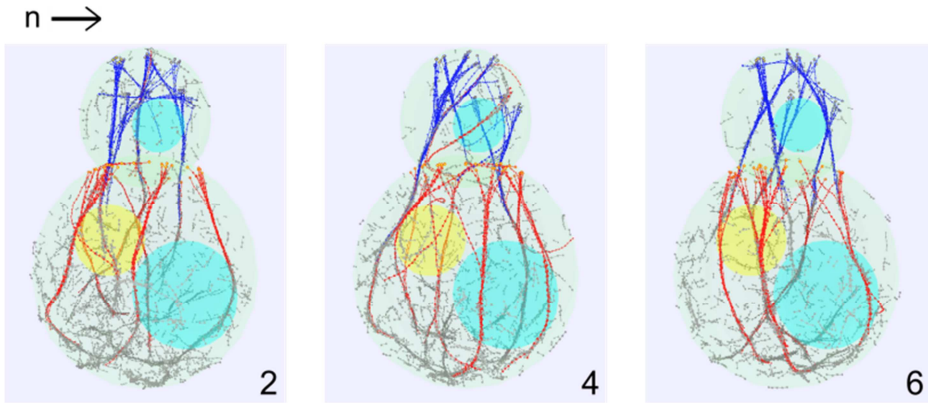

Figure S2. Effect of filament severing cooperativity parameter *n*. In our simulations the actin filament severing rate is described a Hill function with cooperativity coefficient *n*, Equation (3). Higher values of *n* represent stronger cooperativity and the lengths of actin filaments are less variable. Snapshots of simulations at 120 s with *n* varied from 2 to 6, with other parameters from Table I (the value of *n* used in all other simulations in this paper is $n = 6$). There is no significant change in cable structure, however with increased *n* the formin associated actin filaments (red and blue) are less likely to sever at shorter lengths.

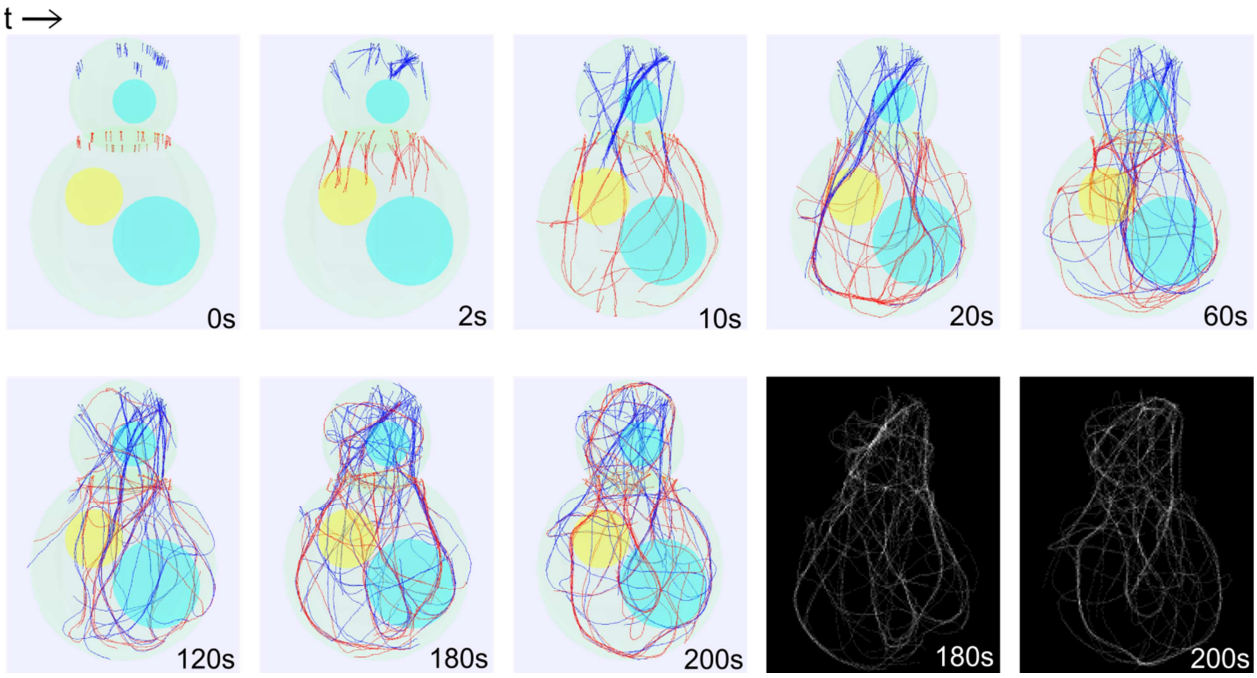

Figure S3. Actin cable formation using the turnover and crosslinking mechanism of [Tang et al., 2014]. Actin cable structures are also seen when using a crosslinking potential (r_c = 0.12 µm and k_c = 2 pN/µm) between filament beads that is not angle-dependent and simulating turnover by removing the whole filament with a rate that corresponds to an average filament length of 6 µm (1/20 s^{-1} for Bni1 filaments and 1/10 s^{-1} for Bnr1 filaments). Lower right panels show two projected images.

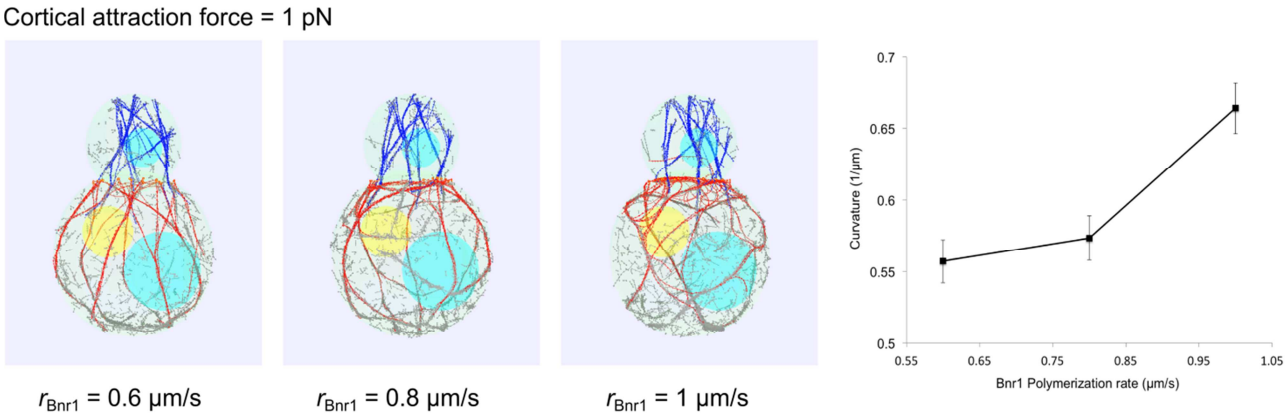

Figure S4. Simulations of increasing Bnr1 formin polymerization rate, including an attractive cortical force to the mother cell boundary of magnitude F^{cortex} = 1 pN. Increase of Bnr1 polymerization rate produces a dense and wavy actin cable network, similar to the simulations and experiments of Figure 5 for *smy1Δ* cells. The addition of cortical force causes the cables to come close to the plasma membrane, as described in Figure 2D, E. The curvature as function of r_{Bnr1} is not significantly altered as compared to the case without cortical attraction in Figure 5. The simulation snapshots are taken at steady state (after 60 s for r_{Bnr1} = 0.6 μm/s and at 50 s for the other two cases). Curvature data used 9 time points starting at 45 s, separated by 5 s, from 3 independent runs. Error bar is one standard deviation.

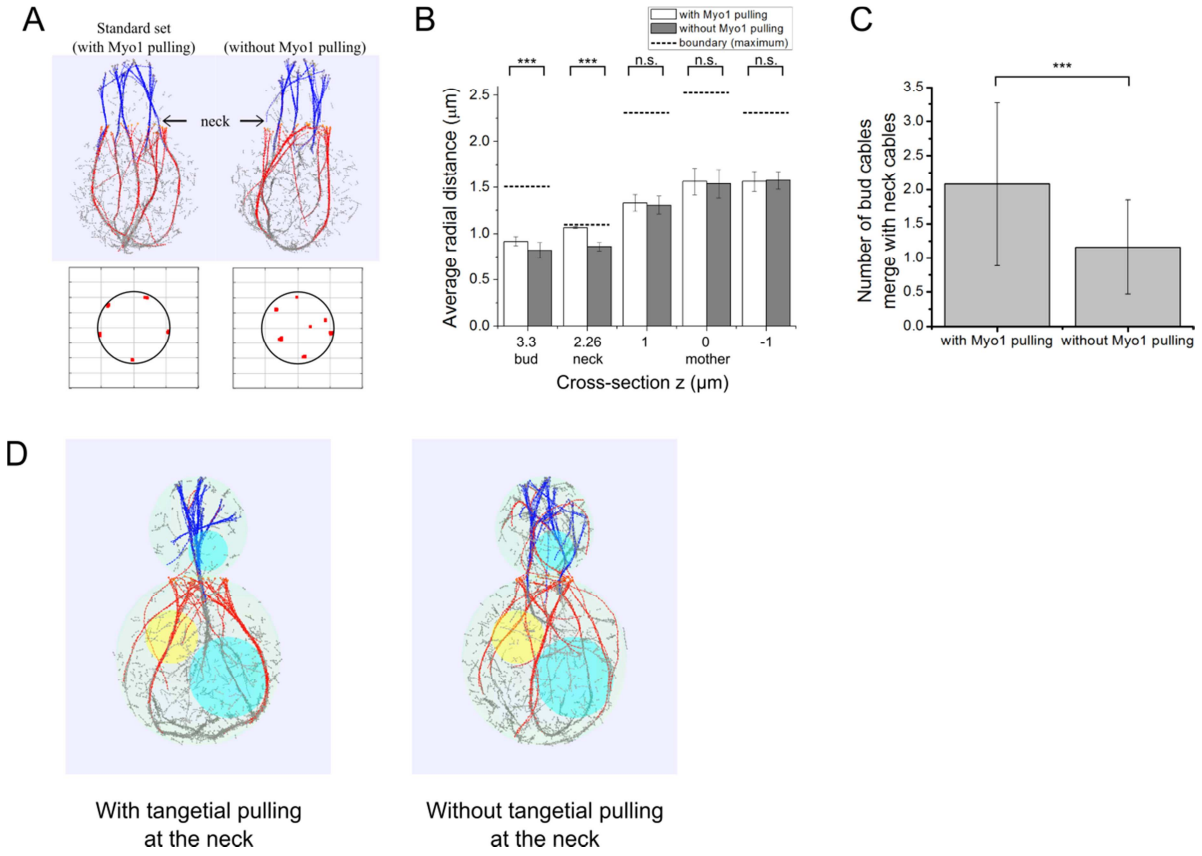

Figure S5. Simulated binding and Myo1 pulling at the neck connects Bni1 associated cables with Bnr1 associated cables. (A) Simulation snapshots of actin cable structures with or without neck binding and Myo1 pulling. Cell boundary, nucleus and vacuoles are not shown. (Lower) Cross-section cut at the neck (z = 2.26 μm) shows the distribution of actin filaments crossing the plane (circle: neck boundary). The neck forces attract the actin cables at the neck area towards the neck boundary. (B) Average radial distance of actin filament beads for five cross-sections (z = 3.3, 2.26, 1, 0, -1 μm) in the bud, at the neck, and in the mother cell (dashed lines show the maximum possible radius at each z, ***: $p < 0.001$, n.s.: not significant). The effect of Myo1 pulling is significant for actin cables at the neck and in the bud, but not in the mother cell. (C) Number of cables in the bud that extend to the mother and merge with the neck cables. Significantly more bud cables connect with neck cables with Myo1 pulling. All error bars in the figure are standard deviations from 15 data points separated by 10 s starting at 80 s, from 3 independent runs. (D) Simulations with small neck radius (0.54 μm) show that Bni1 cables can go through the neck even without the Myo1 pulling, however a larger fraction of filaments remains in the bud without Myo1 pulling. Simulation snapshots taken at 90 s.

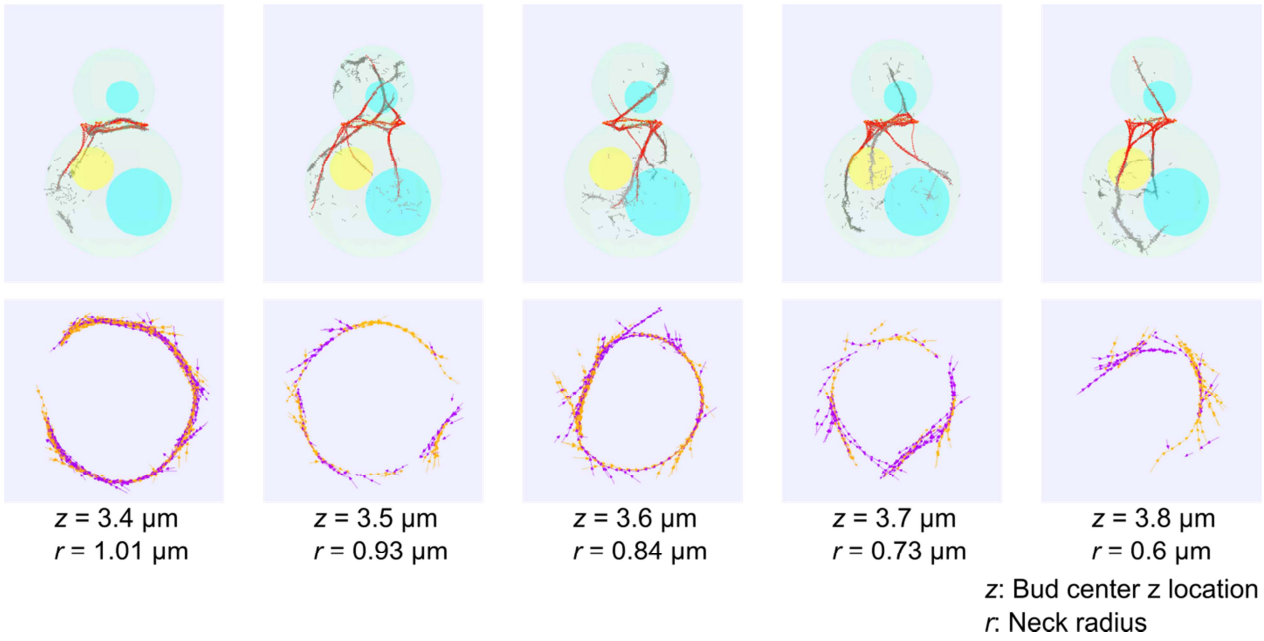

Figure S6. Simulations of actin ring formation for different bud neck radii. Parameters: actin filament elongation rate = 0.3 μm/s and no type V myosin pulling force. The bud center *z* coordinate is varied from 3.4 μm to 3.8 μm, resulting in neck radii varying from 1.01 μm to 0.6 μm. Snapshots of actin filaments (top) and neck plane (bottom) taken at 200 s. Decreasing neck radius destabilizes the ring because filaments at the neck ring need to bend to larger curvatures.

Movies

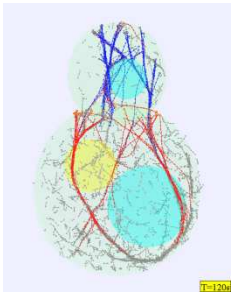

Movie S1. Standard set simulation. Parameters are as described in the Table. Screen captures are obtained every 2 s for a total of 120 s. Budding yeast cell shape is in light green, vacuoles in cyan, nucleus in yellow, Bni1 associated filaments in blue, Bnr1 associated filaments in red, free filaments in gray.

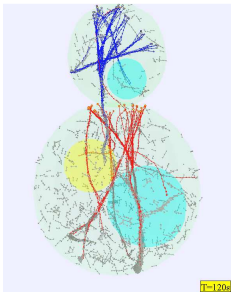

Movie S2. Simulation as in Movie S1, with smaller neck radius. The bud is centered at z = 3.85 µm, generating a bud neck of radius 0.54 µm.

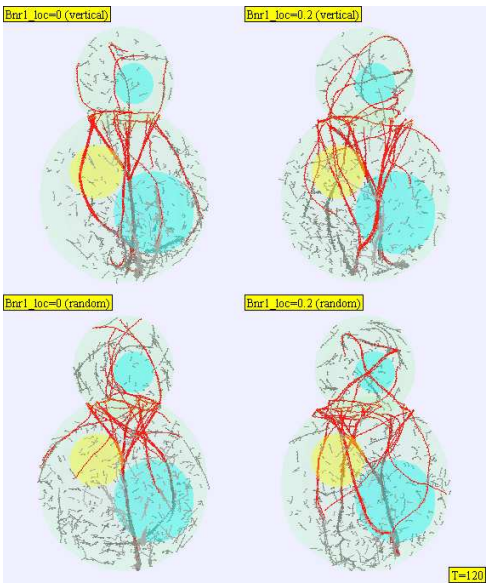

Movie S3. Influence of Bnr1 location and initial direction of filament polymerization in simulations of *bni1Δ* cells. In the two left panels the Bnr1 formins are placed at the neck. The right two panels have the Bnr1 formins at 0.2 µm below the neck, on the mother cell surface. In

the top two panels filaments start to polymerize along the vertical direction. In the bottom panels the initial direction of polymerization is random. In all cases, after a transient, most cables form within the mother cell.

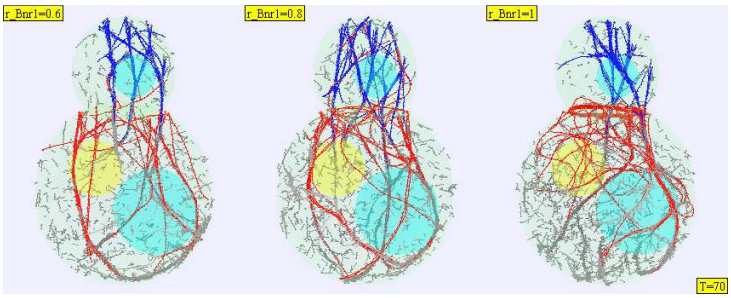

Movie S4. Increase of Bnr1 formin polymerization rate from 0.6 µm/s to 1.0 µm/s reproduces the cable phenotype of *smy1Δ* cells.

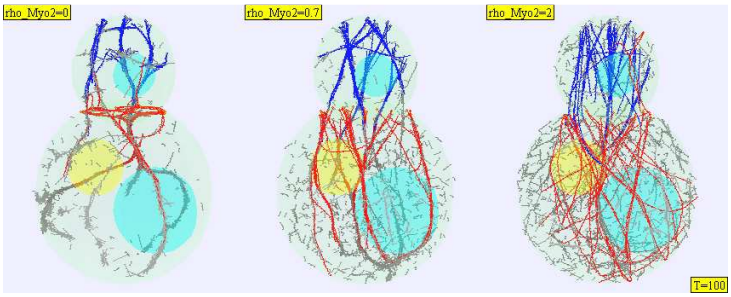

Movie S5. Change in cable structure by increase of myosin V pulling density, ρ_{MyoV}, from 0 to 2/µm.

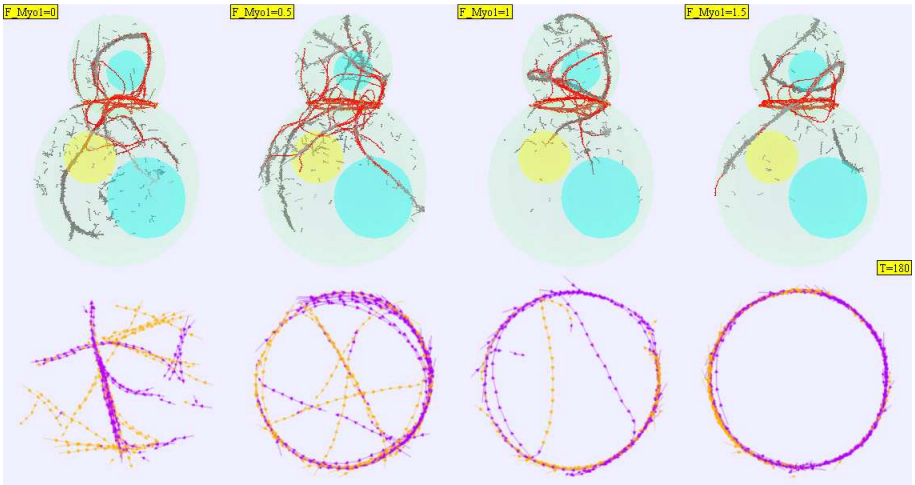

Movie S6. Increase of neck attraction force results in formation of actin ring of antiparallel filaments at the bud neck. The net neck attraction force is increased from 0 to 1.5 pN, in the absence of bud tip formins and type V myosin force (other parameters same as Table I). Bottom row is a cross-section at the neck showing clockwise (purple) and counter-clockwise (orange) oriented filaments.